J|A|C|S
ARTICLES
Published on Web 02/12/2004

Mechanism of Stereo- and Regioselectivity in the Paternò−Büchi Reaction of Furan Derivatives with Aromatic Carbonyl Compounds: Importance of the Conformational Distribution in the Intermediary Triplet 1,4-Diradicals

Manabu Abe,*,† Takanori Kawakami,† Shinji Ohata,† Koichi Nozaki,‡ and Masatomo Nojima†

Contribution from the Department of Materials Chemistry, Graduate School of Engineering, Osaka University (HANDAI), Suita 565-0871, Osaka, Japan, and Department of Chemistry, Graduate School of Science, Osaka University, Toyonaka 560-0043, Osaka, Japan

Received November 7, 2003; E-mail: abe@ap.chem.eng.osaka-u.ac.jp

Abstract: Temperature and substituent effects on the stereo- and regioselectivity have been investigated in the photochemical [2 + 2] cycloaddition reaction, the so-called Paternò−Büchi (PB) reaction, of unsymmetrically substituted furans **2a,b** (2-methyl- and 3-methylfuran) with aromatic carbonyl compounds **1a,b** (benzaldehyde and benzophenone). The regio-random but stereoselective (exo/endo > 97/3) formation of lower substituted oxetane **3a** and higher substituted oxetane **4a** is found in the reaction with benzaldehyde (**1a**). The exclusive stereoselectivity is not dependent on the position of methyl substituent on the furan ring and the reaction temperature. The double-bond selection (**3a** versus **4a**) is slightly dependent on the reaction temperature (**3a**/**4a** = 55/45 to 40/60). The Eyring plots of the regioselectivity are linear. Contrastively, in the reaction with benzophenone (**1b**), the double-bond selection (**3b** versus **4b**) largely depends on the reaction temperature. The Eyring plots are not linear, but the inflection points are observed. The transient absorption spectroscopic analyses (picosecond time scale) clarify the intervention of triplet 2-oxabutane-1,4-diyls in the photochemical processes. Computational studies reveal the equilibrium structures of the triplet diradicals, energy barriers between the conformers, and the equilibrium constants. A rational mechanism is herein proposed by the support of both experimental and computational investigations to account for not only the exclusive formation of the exo-configured oxetanes **3a** and **4a** but also the nonlinear Eyring plots observed in the reaction with **1b**.

Introduction

Schenck[1] first reported the exclusive formation of 2-alkoxy-oxetane, 6,6-diphenyl-2,7-dioxabicyclo[3.2.0]hept-3-ene, in the Paternò−Büchi (PB) photochemical [2 + 2] cycloaddition[2] of furan with benzophenone. After his finding, several chemists explored the regioselectivity[3] (double-bond selection) for the reaction of unsymmetrically substituted furans. The stereoselectivity[4] was also investigated for the reactions with unsymmetrical carbonyl compounds. For example, the exclusive formation of higher substituted oxetane **4** was reported in the reaction of 2-methylfuran (**2a**) or 3-methylfuran (**2b**) with benzophenone (**1b**) at ambient temperature (Scheme 1).[3b,d] In contrast, a regio-random formation of oxetanes **3aa** and **4aa** was found in the reaction with benzaldehyde **1a**,[3a,4h] although the exo-selective formation of the oxetanes was observed (Scheme 1).[4h] The mechanism to interpret the regio- and stereoselectivity is still unclear, though the PB reaction is one of the fundamental photochemical cycloaddition reactions.[4m,5−7] In the present study, we have investigated temperature and substituent effects on the selectivities in the PB reactions that have not been reported thus far.[8] With help of computational calculations, we report here the conclusive mechanism for rationalizing the regio- and stereoselectivity.

Scheme 1. Paternò−Büchi Reaction of Furan Derivatives with Aromatic Carbonyl Compounds

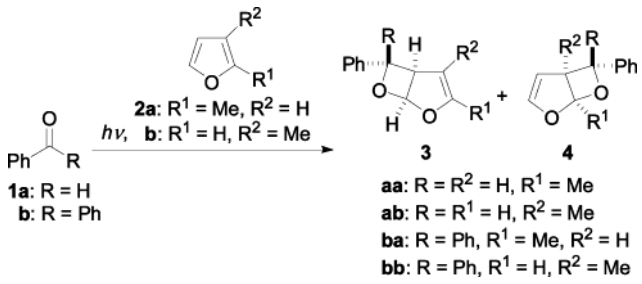

† Graduate School of Engineering, Osaka University.
‡ Graduate School of Science, Osaka University.

(1) Schenck, G. O.; Hartmann, W.; Steinmetz, R. *Chem. Ber*. **1963**, *96*, 498.
(2) (a) Paternò, E.; Chieffi, G. *Gazz. Chim. Ital*. **1909**, *39*, 341. (b) Büchi, G.; Inman, C. G.; Lipinsky, E. S. *J. Am. Chem. Soc*. **1954**, *76*, 4327.
(3) (a) Toki, S.; Shima, K.; Sakurai, H. *Bull. Chem. Soc. Jpn*. **1965**, *38*, 760. (b) Rivas, C.; Payo, E. *J. Org. Chem*. **1967**, *32*, 2918. (c) Sakurai, H.; Shima, K.; Toki, S. *Nippon Kagaku Zasshi* **1968**, *89*, 537. (d) Nakano, T.; Rivas, C.; Perez, C. *J. Chem. Soc., Perkin Trans. 1* **1973**, 2322. (e) Schreiber, S. L.; Desmaele, D.; Porco, J. A., Jr. *Tetrahedron Lett*. **1988**, *51*, 6689. (f) Carless, H. A.; Halfhide, F. E. *J. Chem. Soc., Perkin Trans. 1* **1992**, 1081. (g) D'Auria, M.; Racioppi, R.; Romaniello, G. *Eur. J. Org. Chem*. **2000**, 3265.

10.1021/ja039491o CCC: $27.50

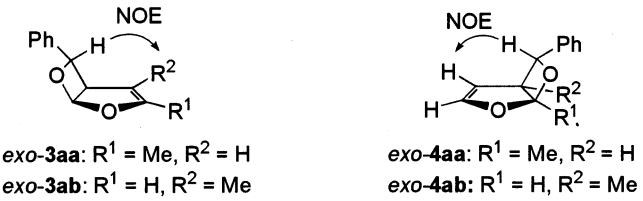

exo-**3aa**: R^1 = Me, R^2 = H
exo-**3ab**: R^1 = H, R^2 = Me
exo-**4aa**: R^1 = Me, R^2 = H
exo-**4ab**: R^1 = H, R^2 = Me

Figure 1. Structural determination of exo-oxetanes **3** and **4**.

Results

Photoreaction of 2-Methylfuran (2a) with Aromatic Carbonyl Compounds 1a and 1b. A degassed toluene solution of freshly distilled 2-methylfuran (**2a**, 0.50 M) and aromatic carbonyl compounds **1a** or **1b** (0.05 M) was irradiated with a high-pressure Hg lamp (300 W, $h\nu$ > 300 nm) through a Pyrex filter (Scheme 1). To avoid the formation of bisoxetanes[9] by the reaction of **1** with the bicyclic monooxetane **3** and/or **4**, the irradiation was stopped at the stage of ca. 30% conversion of the carbonyl compounds. Under the reaction conditions only oxetanes **3** and **4** (total yields > 95%) were detected as photoprimary products, which were carefully analyzed by ^{1}H NMR (600 or 270 MHz) spectroscopy. Thus, it was feasible to determine accurately the product ratios by comparing the ^{1}H NMR peak areas of the isomeric oxetanes, error ±3%.

In the photoreaction with **1a**, two regioisomeric oxetanes **3aa** (R = R^2 = H, R^1 = Me) and **4aa** (R = R^2 = H, R^1 = Me) were observed in the photolyzate. The product structures were confirmed by the ^{1}H and ^{13}C NMR (DEPT) spectroscopic analyses. The exo-configuration of the oxetanes was unequivocally determined by the ^{1}H NMR (600 MHz) NOE measurements (Figure 1).

In the reactions, we could not detect any trace of the endo-isomers (<3%) by means of ^{1}H NMR (600 MHz) spectroscopic analyses. The highly exo-selective formation of the oxetanes (quantum yield, Φ_{3+4} = 0.31−0.45) was observed in the temperature range (−76 to +52 °C) under investigation (Figure 2a). The Eyring plot[10] of the regioselectivity, ln(**3aa**/**4aa**) against 1/*T*, is shown in Figure 2a. The regioselectivity was linearly changed with varying reaction temperature. The activation parameters, $\Delta\Delta H^{\ddagger}$ = −0.24 kcal/mol and $\Delta\Delta S^{\ddagger}$ = −1.1 cal/Kmol, were determined from the slope and intercept of the linear plot.

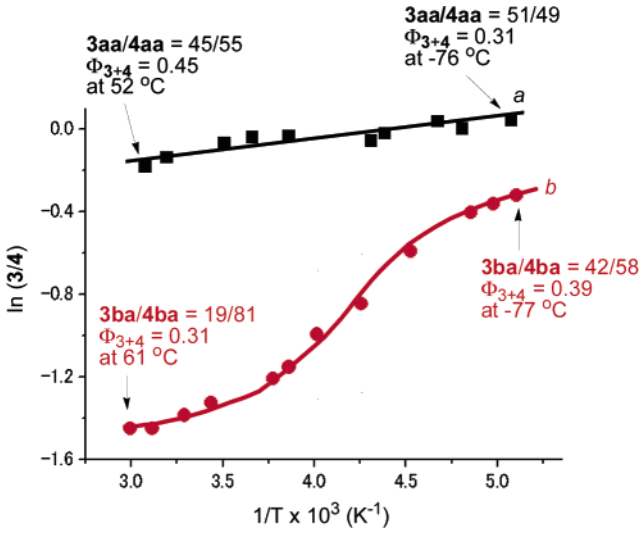

Figure 2. Eyring plots of regioselectivity, ln(**3**/**4**) against 1/*T* (K^{-1}), in the photoreaction of 2-methylfuran (**2a**) with (a) ■ benzaldehyde (**1a**), exo/endo > 97/3 and (b) ● benzophenone (**1b**).

As for the photoreaction of **2a** with **1b**, the regioselectivity **3ba** (R = Ph, R^1 = Me, R^2 = H) versus **4ba** (R = Ph, R^1 = Me, R^2 = H) was largely dependent on the reaction temperature (Figure 2b). Thus, regioisomers **3ba** and **4ba** (isomer ratio 42/58) were obtained at −77 °C in high yields (>95%, Φ_{3+4} = 0.39). However, the selective formation of higher substituted oxetane **4ba** was observed at 61 °C, and the product ratio was **3ba**/**4ba** = 19/81 (Φ_{3+4} = 0.31). It should be noted that the Eyring plot for the regioselectivity was not linear but *S*-shaped (Figure 2b). The nonlinear Eyring plots clearly indicate that the selectivity-determining step varies during the change in the reaction temperature (vide infra).[11]

Photoreaction of 3-Methylfuran (2b) with Aromatic Carbonyl Compounds 1a and 1b. The temperature effect on the regioselectivity in the photoreaction of 3-methylfuran (**2b**) was also investigated under the similar conditions mentioned above for the reaction of **2a**. The stereoselective formation (Φ_{3+4} = 0.23−0.28) of exo-configured oxetanes **3ab** (R = R^1 = H, R^2 = Me) and **4ab** (R = R^1 = H, R^2 = Me) was found in the reaction with **1a** (Figure 1). The diastereoselectivity (>94% de) was independent of the reaction temperature. As observed in the reaction of **2a**, the Eyring plot for the regioselectivity was linear (Figure 3a). From the slope and intercept, the activation parameters were determined to be $\Delta\Delta H^{\ddagger}$ = −0.58 kcal/mol and $\Delta\Delta S^{\ddagger}$ = −2.7 cal/Kmol.

In sharp contrast to the temperature effect on the regioselectivity observed in the reaction of **2a** with **1b** (Figure 2b), the product ratio of **3bb**/**4bb** in the reaction of **2b** nonlinearly increased with the increase of the reaction temperature (Figure 3b). Thus, at low temperatures (ca. <−20 °C), the regioselectivity (**3bb**/**4bb**) was around 17/83, whereas the ratio was 34/66 at +56 °C. It should be noted that the quantum yield, Φ_{3+4}, for the oxetane formations was largely dependent on the reaction temperature. Thus, the yield drastically decreased with the increase of the reaction temperature: 0.39 (at −77 °C) → 0.06 (at +56 °C).

(4) (a) Shima, K.; Sakurai, H. *Bull. Chem. Soc. Jpn.* **1966**, *39*, 1806. (b) Whipple, E. B.; Evanega, G. R. *Tetrahedron* **1968**, *24*, 1299. (c) Jarosz, S.; Zamojski, A. *Tetrahedron* **1982**, *38*, 1447. (d) Jarosz, A.; Zamojski, A. *Tetrahedron* **1982**, *38*, 1453. (e) Schreiber, S. L.; Hoveyda, A. H.; Wu, H.-J. *J. Am. Chem. Soc.* **1983**, *105*, 660. (f) Schreiber, S. L.; Satake, K. *J. Am. Chem. Soc.* **1983**, *105*, 6723. (g) Schreiber, S. L.; Hoveyda, A. H. *J. Am. Chem. Soc.* **1984**, *106*, 7200. (h) Schreiber, S. L.; Porco, J. A., Jr. *J. Org. Chem.* **1989**, *54*, 4721. (i) Cantrell, T. S.; Allen, A. C.; Ziffer, H. *J. Org. Chem.* **1989**, *54*, 140. (j) Hambalek, R.; Just, G. *Tetrahedron Lett.* **1990**, *31*, 4693. (k) Hambalek, R.; Just, G. *Tetrahedron Lett.* **1990**, *31*, 5445. (l) Griesbeck, A. G.; Mauder, H.; Peters, K.; Peters, E.-M.; Schnering, H. G. *Chem. Ber.* **1991**, *124*, 407. (m) Griesbeck, A. G.; Buhr, S.; Giege, M.; Schmickler, H.; Lex, J. *J. Org. Chem.* **1998**, *63*, 3847. (n) Hu, S.; Neckers, D. C. *J. Chem. Soc., Perkin Trans. 2* **1999**, 1771. (o) Zhang, Y.; Xue, J.; Gao, Y.; Fun, H.-K.; Xu, J.-H. *J. Chem. Soc., Perkin Trans. 1* **2002**, 345.
(5) Toki, S.; Sakurai, H. *Bull. Chem. Soc. Jpn.* **1967**, *40*, 2885.
(6) Abe, M.; Torii, E.; Nojima, M. *J. Org. Chem.* **2000**, *65*, 3426.
(7) Abe, M. In *Organic Photochemistry and Photobiology*, 2nd ed.; Horspool, W., Lenci, F., Eds.; CRC Press: Boca Raton, FL, 2004; Chapter 62.
(8) In ref 3a,b, the exclusive formation of more-substituted oxetane **4** was reported, but in this study the regioselectivity has been found to largely depend on the reaction temperature.
(9) (a) Ogata, M.; Watanabe, H.; Kano, H. *Tetrahedron Lett.* **1967**, 533. (b) Letich, J. *Tetrahedron Lett.* **1967**, 1937. (c) Evanega, G. R.; Whipple, E. B. *Tetrahedron Lett.* **1967**, 2163. (d) Toki, S.; Sakurai, H. *Tetrahedron Lett.* **1967**, 4119.
(10) Eyring, H. *J. Chem. Phys.* **1935**, *3*, 107.
(11) (a) Bushmann, H.; Scharf, D. N.; Hoffmann, N. *Angew. Chem., Int. Ed. Engl.* **1991**, *30*, 47. (b) Göbel, T.; Scharpless, K. B. *Angew. Chem., Int. Ed. Engl.* **1993**, *32*, 1329. (c) Hale, K. J.; Ridd, J. H. *J. Chem. Soc., Chem. Commun.* **1995**, 357. (d) Gypser, A.; Norrby, P.-O. *J. Chem. Soc., Perkin Trans. 2* **1997**, 939.

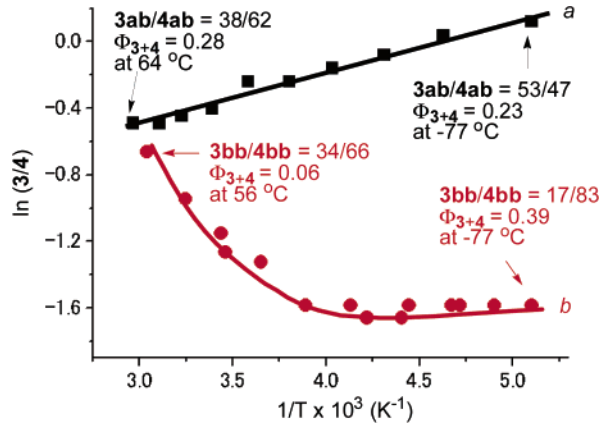

Figure 3. Eyring plots of regioselectivity, ln(**3**/**4**) against $1/T$ (K^{-1}), in the photoreaction of 3-methylfuran (**2b**) with (a) ■ benzaldehyde (**1a**), exo/endo > 97/3 and (b) ● benzophenone (**1b**).

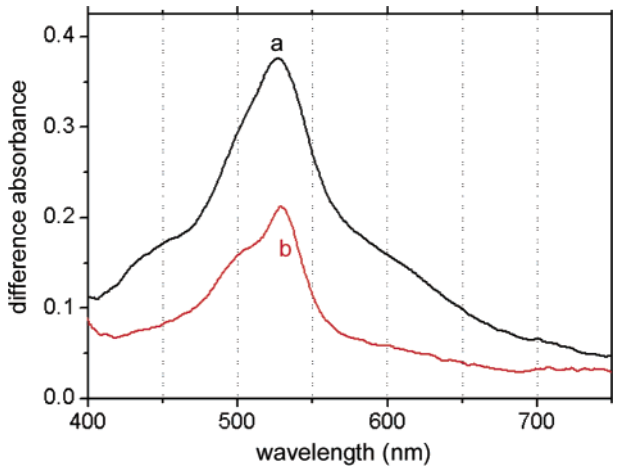

Figure 4. Transient absorption spectra of (a) triplet benzophenone **1b*** and (b) triplet 1,4-diradicals **T-DR3ba** and/or **T-DR4ba** formed in the irradiation of 5 M 2-methylfuran (**2a**) with 0.025 M benzophenone (**1b**) in acetonitrile at 1000 ps.

Transient Absorption Spectroscopy. Nonlinear Eyring plots (Figure 2b and 3b) clearly suggest that oxetanes **3** and **4** are formed in the reaction of two or more steps.[11] To get information of the intermediates in the PB reactions, transient absorption spectra were measured for the reactions with **1b** on a picosecond time scale (λ_{exc} = 355 nm, 20 ps pulse width). The diphenyl chromophore was expected to make it possible to detect transient species in visible regions. In the absence of a furan derivative, the triplet state of benzophenone **1b*** (τ > 1 μs,[12] λ_{max} = 525 nm[13]) was observed within 20 ps after the laser excitation in degassed acetonitrile (Figure 4a). As shown in Figure 4b, upon the addition of 5 M acetonitrile solution of 2-methylfuran (**2a**), the transient species **1b*** was quenched within 500 ps to generate new species with an absorption maximum (λ_{max}) at 531 nm. The transient species decayed with almost first-order kinetics (τ = ca. 4.5 ns, $k_d = 2.1 \times 10^8$ s^{-1}) at 25 °C. The absorption spectrum in the visible region of the new species is similar to that of the triplet 1,1-diphenyl-2-oxabutane-1,4-diyl **DR** (λ_{max} = 535 nm, τ = 1.5 ns in acetonitrile) reported in the photoreaction of 1,4-dioxene with benzophenone.[14] Therefore, it is reasonable to conclude that the new species are triplet 1,4-diradicals **T-DR3ba** and/or **T-DR4ba** (Scheme 4). In the photoreaction of **2b** with **1b**, the quite similar transient absorption spectrum was observed (λ_{max} 530 nm, $k_d = 3.9 \times 10^8$ s^{-1}), which is also assigned to the triplet diradicals **T-DR3bb** and/or **T-DR4bb**.

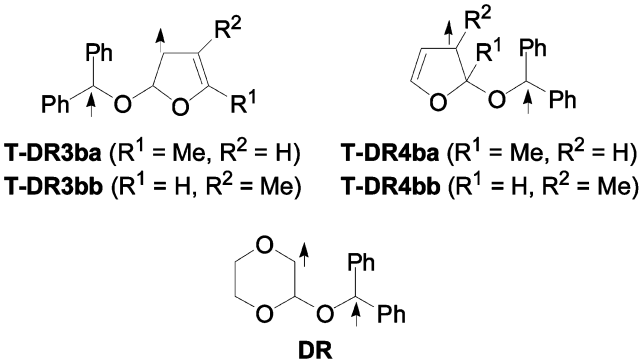

In the following section, we will discuss the mechanism for the exo-selective formation of oxetanes **3** and **4** in the reaction with **1a** and for the regioselectivity (nonlinear Eyring plots) in the reaction with **1b**.

Discussion

exo-Selective Formation of Oxetanes 3 and 4. As observed for the PB reaction with benzophenone (**1b**), triplet 2-oxabutane-1,4-diyls **T-DR3a** and **T-DR4a** are also proposed to be the intermediates for the formation of exo-oxetanes **3** and **4** in the reaction with **1a** (Scheme 2). The intersystem crossing (ISC) process to singlet is necessary so that triplet diradicals may give products. Since the lifetime of singlet diradicals is usually quite short,[15] the conformations of their precursor, triplet diradicals, play an important role to determine the product selectivity (memory effect).[16−19] To get information on the mechanism for the exclusive formation of exo-oxetanes **3** and **4**, potential energy surfaces (PES) around the dihedral angle θ (deg) were calculated for both **T-DR3a** and **T-DR4a** at the UB3LYP/6-31G* level of theory[20] with GAUSSIAN 98[21] suite of programs (Figure 5). Among the possible conformers of **T-C1a**−**C3a** in **T-DR3a** and **T-C1a′**−**C3a′** in **T-DR4a**, only four conformers, inside-gauche conformers **T-C1a** and **T-C1a′** (θ = ca. 60°) and outside-anti conformers **T-C2a** and **T-C2a′** (θ = ca. 180°), were calculated to be energy minimum structures. The outside-gauche conformers, **T-C3a** and **T-C3a′** (θ = ca. 300°), did not exist as equilibrium structures. The energetic preference of the inside-gauche and outside-anti conformers is reasonably explained by

(12) Poter, G.; Wilkinson, F. *Trans. Faraday Soc.* **1962**, *58*, 1686.
(13) Green, B. I.; Hockstrasser, R. M.; Weisman, R. *J. Chem. Phys.* **1979**, *70*, 1247.
(14) (a) Freilich, S. C.; Peters, K. S. *J. Am. Chem. Soc.* **1981**, *103*, 6255. (b) Freilich, S. C.; Peters, K. S. *J. Am. Chem. Soc.* **1985**, *107*, 3819.
(15) For unusually long-lived singlet diradicals, see: (a) Adam, W.; Borden, W. T.; Burda, C.; Foster, H.; Heidenfelder, T.; Jeubes, M.; Hrovat, D. A.; Kita, F.; Lewis, S. B.; Scheutzow, D.; Wirz, J. *J. Am. Chem. Soc.* **1998**, *120*, 593. (b) Abe, M.; Adam, W.; Heidenfelder, T.; Nau, W. M.; Zhang, X. *J. Am. Chem. Soc.* **2000**, *122*, 2019. (c) Abe, M.; Adam, W.; Hara, M.; Hattori, M.; Majima, T.; Nojima, M.; Tachibana, K.; Tojo, S. *J. Am. Chem. Soc.* **2002**, *124*, 6540.
(16) Giese, B.; Wetstein, P.; Stahelin, C.; Barnosa, F.; Neuburger, M.; Zehnder, M.; Wessig, P. *Angew. Chem., Int. Ed.* **1999**, *38*, 2586.
(17) Scaiano, J. C. *Tetrahedron* **1982**, *38*, 819.
(18) (a) Wagner, P. J. *Acc. Chem. Res.* **1989**, *22*, 83. (b) Zand, A.; Park, B.-S.; Wagner, P. J. *J. Org. Chem.* **1997**, *62*, 2326.
(19) (a) Griesbeck, A. G.; Stadtmüller, S. *J. Am. Chem. Soc.* **1990**, *112*, 1281. (b) Griesbeck, A. G.; Stadtmüller, S. *J. Am. Chem. Soc.* **1991**, *113*, 6923. (c) Griesbeck, A. G.; Mauder, H.; Stadtmüller, S. *Acc. Chem. Res.* **1994**, *27*, 70.
(20) (a) Becke, A. D. *J. Chem. Phys.* **1993**, *98*, 5648. (b) Lee, C.; Yang, W.; Parr, R. G. *Phys. Rev. B* **1988**, *37*, 785. (c) Hariharan, P. C.; Pople, J. A. *Theor. Chim. Acta* **1973**, *28*, 212.

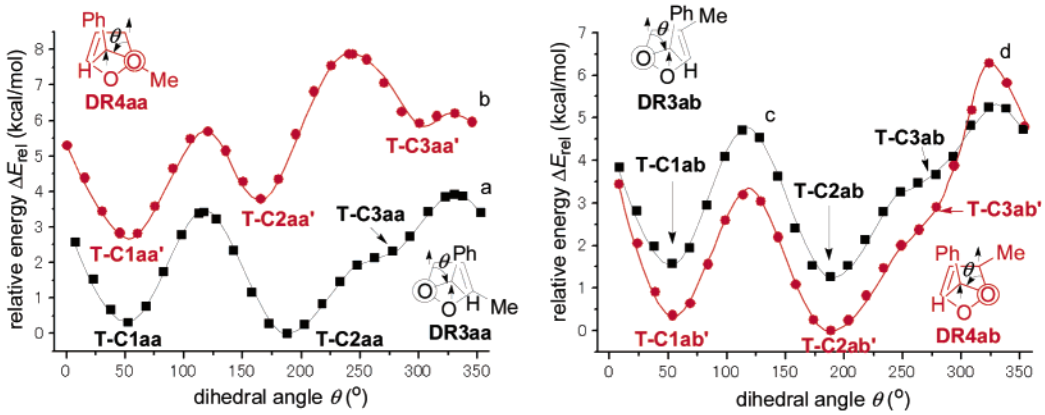

Figure 5. PES analyses around the dihedral angle (θ°) of diradicals (a) **T-DR3aa**, (b) **T-DR4aa**, (c) **T-DR3ab**, and (d) **T-DR4ab**. The energies, ΔE_{rel} in kcal/mol, were relative to the most stable conformer.

Scheme 2. Mechanism for the Selective Formation of exo-Oxetanes **3a** and **4a** in the Photoreaction of Furans **2a,b** with Benzaldehyde (**1a**)

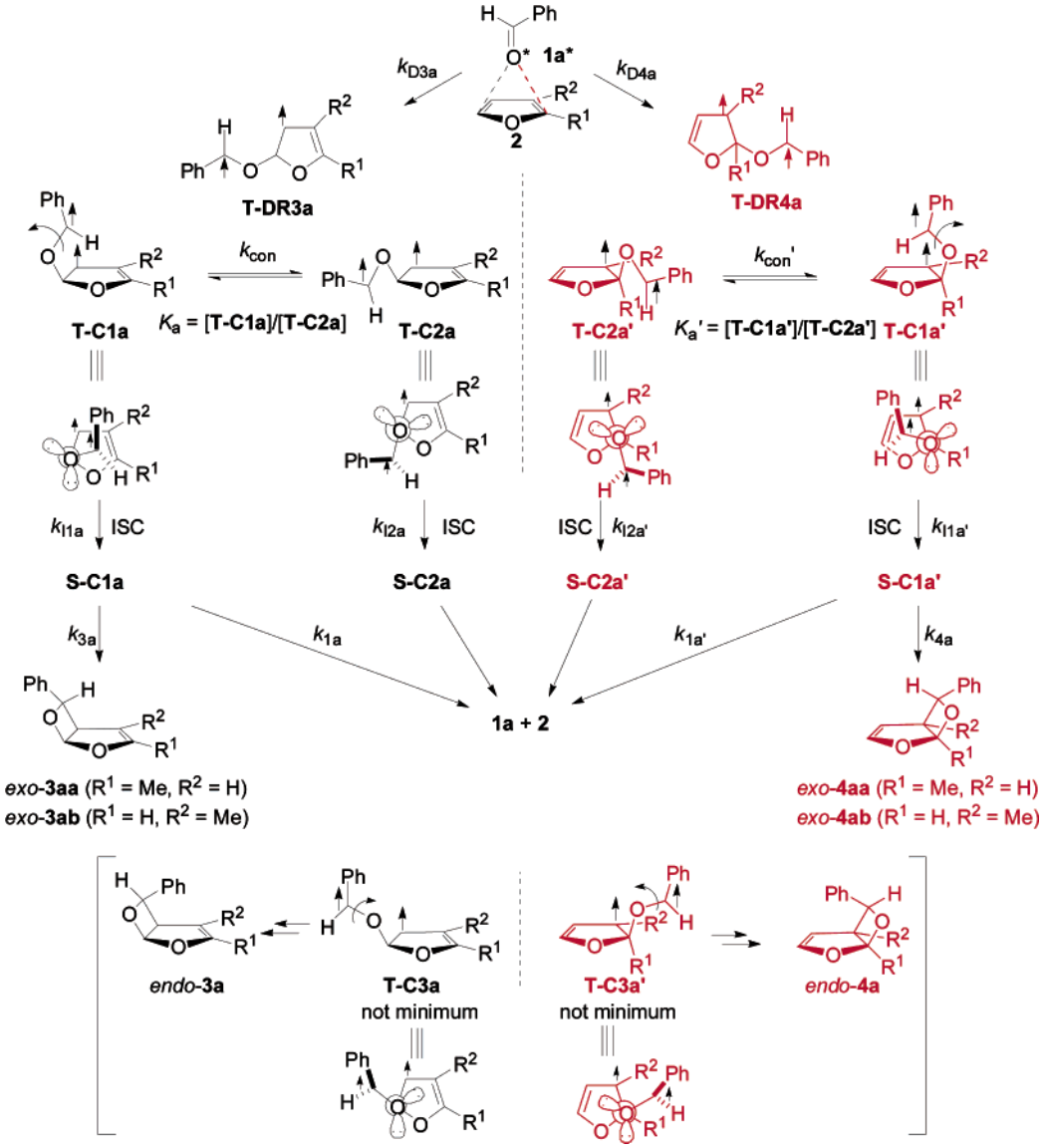

stereoelectronic effect, i.e., gauche effect,[22] on the conformational stability of the ketals. Thus, the orbital overlap of *n* orbital of oxygen with σ^* orbital of the C−O bond in the furan ring is quite effective in the four conformers, **T-C1a**, **T-C2a**, **T-C1a′**, and **T-C2a′**. However, the overlap is very poor in the conformers of **T-C3a** and **T-C3a′** (Scheme 2). The phenyl ring in the optimized structures of intermediary triplet diradicals **T-DR3a** and **T-DR4a** is located to be perpendicular to the furan ring, as exemplified for **T-C1aa** (Scheme 3). The energetic preference of the perpendicular orientation is reasonably explained by the

Scheme 3. Selective Formation of exo-Oxetane **3aa** by the Outward Rotation of the Phenyl Ring in the Intermediary Triplet Diradical **T-C1aa**

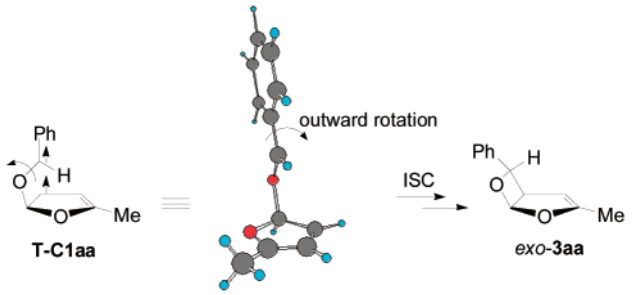

orbital interaction between 2p AO of oxygen and the radical p-orbital of the benzyl radical part.[23] According to the memory effect, the inside-gauche conformers, **T-C1a** and **T-C1a′**, are expected to give *exo*-**3a** and *exo*-**4a** by the *outward* rotation of the phenyl group; see the curved arrow in **T-C1a** and **T-C1a′** (Schemes 2 and 3).[24] The outside-gauche conformers **T-C3a** and **T-C3a′** may afford endo-isomers *endo*-**3a** and *endo*-**4a** by the *inward* rotation of the phenyl group. The anti-conformers **T-C2a** and **T-C2a′** go back to the starting compounds **1a** and **2** after the ISC process to the singlet states. The PES analyses (Figure 5) clearly suggest that among the productive conformers only inside-gauche conformers **T-C1a** and **T-C1a′** exist as energy minimum structures. Thus, the exclusive formation of the exo-oxetanes is expected in the PB reactions, and the stereoselectivity should be temperature-independent. In fact, we did observe the highly exo-selective formation of the oxetanes **3** and **4**, and the stereoselectivities were temperature-independent.

As for regioselectivity (**3** versus **4**), the Eyring plots of the reaction with **1a** were linear (Figures 2a and 3a). There are four factors that determine the regioselectivity (Scheme 2): (i) Initial double bond selection by triplet benzaldehyde, k_{D3a} versus k_{D4a}, (ii) equilibrium constants, $K_a = [\mathbf{T\text{-}C1a}]/[\mathbf{T\text{-}C2a}]$ versus $K_a' = [\mathbf{T\text{-}C1a'}]/[\mathbf{T\text{-}C2a'}]$, (iii) relative rate constant of the ISC processes in the triplet 1,4-diradicals, k_{I1a}/k_{I2a} versus $k_{I1a'}/k_{I2a'}$, and (iv) relative rate constant of the bond-forming and bond-breaking step from the singlet 1,4-diradicals **S-C1a** and **S-C1a′**, k_{3a}/k_{1a} versus $k_{4a}/k_{1a'}$. As shown in Figure 5, the energy barriers on the triplet energy surfaces between the inside-gauche (**T-C1a** and **T-C1a′**) and outside-anti conformers (**T-C2a** and **T-C2a′**) are calculated to be around 3 kcal/mol. Thus, the conformational changes between the two conformers are expected to be very fast in the temperature range under investigations, $k_{con} > 10^{\sim 9-10}\ s^{-1}$. The rate constant ($k_I$) of the ISC processes from the triplet to the singlet diradicals, which are spin-forbidden process,[25] are estimated to be around $10^8\ s^{-1}$, as observed for diradicals **T-DR3b** and **T-DR4b** (R = Ph) (Figure 4). Thus, the conformational changes between the inside-gauche and outside-anti conformers are expected to be faster than the ISC processes. According to the Curtin−Hammett principle,[26] the ratios of the productive conformers **S-C1a** and **S-C1a′** are determined not only by the populations of **T-C1a** and **T-C1a′** but also by the relative rate constant of the ISC processes, k_{I1a}/k_{I2a} and $k_{I1a'}/k_{I2a'}$. Since in general the rate constant of ISC processes are insensitive to temperature,[18a,27] the ratios of k_{I1a}/k_{I2a} and $k_{I1a'}/k_{I2a'}$ would be independent of the reaction temperature.[28] When the difference between the two ratios is negligible ($k_{I1a}/k_{I2a} \approx k_{I1a'}/k_{I2a'}$), the regioselectivity (**3a**/**4a**) can be simply determined by the difference of the rate constants between the initial double-bond selection (k_{D3a} versus k_{D4a}) and the equilibrium constants (K_a and K_a') (eq 1). The equation is applied under the condition of $k_{3a}/k_{1a} = k_{4a}/k_{1a'}$. When the ratio of the two rate constants is largely different, the regioselectivity is determined by eq 2. Even under such conditions, the Eyring plots should be linear as long as the conformational changes are faster than the ISC processes ($k_{con} > k_I$). This mechanism rationalizes the linear Eyring plots observed in the PB reaction of benzaldehyde, despite going through the intermediary triplet diradicals **T-DR3a** and **T-TD4a**.

$$k_{con} > k_I$$

$$\mathbf{3a}/\mathbf{4a} = \frac{k_{D3a}}{k_{D4a}} \times \frac{\dfrac{K_a}{K_a + 1}}{\dfrac{K_a'}{K_a' + 1}} \qquad (1)$$

$$\mathbf{3a}/\mathbf{4a} = \frac{k_{D3a}}{k_{D4a}} \times \frac{\dfrac{K_a}{K_a + 1}}{\dfrac{K_a'}{K_a' + 1}} \times \frac{\dfrac{k_{3a}}{k_{3a} + k_{1a}}}{\dfrac{k_{4a}}{k_{4a} + k_{1a'}}} \qquad (2)$$

Nonlinear Eyring Plots in the PB Reaction of Benzophenone (1b). Scharf and Hoffmann first reported nonlinear Eyring plots in enantioselectivity in PB reactions.[29] Griesbeck and co-workers have also found nonlinear Eyring plots in diastereoselectivity of PB reactions of aliphatic aldehydes. The nonlinearity found by Griesbeck was reasonably explained by the temperature-dependent change of spin state of excited aldehydes (singlet versus triplet) that react with alkenes.[28,30] However, the mechanism of nonlinear Eyring plots is still unclear in PB reactions initiated by pure triplet state of carbonyl compounds. In the present study, we have found nonlinear Eyring plots of

(21) Frisch, M. J.; Trucks, G. W.; Schlegel, H. B.; Scuseria, G. E.; Robb, M. A.; Cheeseman, J. R.; Zakrzewski, V. G.; Montgomery, J. A., Jr.; Stratmann, R. E.; Burant, J. C.; Dapprich, S.; Millam, J. M.; Daniels, A. D.; Kudin, K. N.; Strain, M. C.; Farkas, O.; Tomasi, J.; Barone, V.; Cossi, M.; Cammi, R.; Mennucci, B.; Pomelli, C.; Adamo, C.; Clifford, S.; Ochterski, J.; Petersson, G. A.; Ayala, P. Y.; Cui, Q.; Morokuma, K.; Malick, D. K.; Rabuck, A. D.; Raghavachari, K.; Foresman, J. B.; Cioslowski, J.; Ortiz, J. V.; Stefanov, B. B.; Liu, G.; Liashenko, A.; Piskorz, P.; Komaromi, I.; Gomperts, R.; Martin, R. L.; Fox, D. J.; Keith, T.; Al-Laham, M. A.; Peng, C. Y.; Nanayakkara, A.; Gonzalez, C.; Challacombe, M.; Gill, P. M. W.; Johnson, B. G.; Chen, W.; Wong, M. W.; Andres, J. L.; Head-Gordon, M.; Replogle, E. S.; Pople, J. A. *Gaussian 98*, revision A 11.3; Gaussian, Inc.: Pittsburgh, PA, 1998.
(22) *The Anomeric Effect and Associated Stereoelectronic Effects*; Thatcher, G. R. J., Ed.; ACS Symposium Series 539; American Chemical Society: Washington, DC, 1993.
(23) Palmer, I. J.; Ragazos, I. N.; Bernardi, F.; Olivucci, M.; Robb, M. A. *J. Am. Chem. Soc.* **1994**, *116*, 2121.
(24) Kutateladze, A. G. *J. Am. Chem. Soc.* **2001**, *123*, 9279.
(25) (a) Johnston, L. J.; Scaiano, J. C. *Chem. Rev.* **1989**, *89*, 521. (b) Adam, W.; Grabowski, S.; Wilson, R. M. *Acc. Chem. Res.* **1990**, *23*, 165.
(26) (a) Curtin, D. Y. *Rec. Chem. Prog.* **1954**, *15*, 111. (b) Seeman, J. I. *Chem. Rev.* **1983**, *83*, 83.
(27) (a) Turro, N. J.; Renner, C. A.; Waddell, W. H.; Katz, T. J. *J. Am. Chem. Soc.* **1976**, *98*, 4320. (b) Chang, M. H.; Dougherty, D. A. *J. Am. Chem. Soc.* **1982**, *104*, 2333. (c) Jain, R.; McElwee-White, L.; Dougherty, D. A. *J. Am. Chem. Soc.* **1988**, *110*, 552.
(28) Griesbeck and co-workers have recently reported a temperature-independent diastereoselectivity: Griesbeck, A. G.; Bondock, S.; Gudipati, M. S. *Angew. Chem., Int. Ed.* **2001**, *40*, 4684.
(29) Buschmann, H.; Scharf, H.-D.; Hoffmann, N.; Plath, M. W.; Runsink, J. *J. Am. Chem. Soc.* **1989**, *111*, 5367.
(30) Griesbeck, A. G.; Fiege, M.; Bondock, S.; Gudipati, M. S. *Org. Lett.* **2000**, *2*, 3623.

the regioselectivities (**3ba**/**4ba** and **3bb**/**4bb**) in the pure triplet PB reaction with **1b** (Figures 2b and 3b). Furthermore, the temperature effect on the regioselectivities (**3ba**/**4ba** versus **3bb**/**4bb**) largely depends on the position of the methyl substituent on the furan ring. Thus, the product ratio of **3ba**/**4ba** in the reaction of 2-methylfuran (**2a**) nonlinearly *decreased* with the increase of the reaction temperature (Figure 2b). Alternatively, in the reaction of 3-methylfuran (**2b**) the product ratio of **3bb**/**4bb** nonlinearly *increased* with the increase of the reaction temperature (Figure 3b).

The proposed mechanism for the formation of oxetanes **3b** and **4b** is shown in Scheme 4. The transient absorption spectra mentioned before (Figure 4) strongly support the generation of triplet diradicals **T-DR3b** and **T-DR4b** in the photochemical processes. As discussed in the regioselectivity (**3a** versus **4a**) of the reaction with **1a** (Scheme 2), if the conformational change between the productive conformer (**T-C1b** or **T-C1b′**) and the nonproductive conformer (**T-C2b** or **T-C2b′**) is faster than the ISC process to the singlet diradicals, the Eyring plots of the regioselectivities (**3ba**/**4ba** and **3bb**/**4bb**) should be linear.

Although temperature effect on the ISC process (k_I) is small,[17,27] the rate constants (k_{con}) of conformational changes are temperature-sensitive. The regioselectivity (**3b**/**4b**) can be determined by eq 3 under the conditions that the ISC processes from the triplet diradicals **T-DR3b** and **T-DR4b** to the singlet states overcome the conformational changes of the triplet diradicals at low temperatures, $k_I > k_{con}$ (mechanism I).

Mechanism I: At low temperatures:

$$k_I > k_{con}$$

$$\mathbf{3b}/\mathbf{4b} = \frac{k_{D3b}}{k_{D4b}} \times \left(\frac{k_{3b}}{k_{3b} + k_{1b}} \Big/ \frac{k_{4b}}{k_{4b} + k_{1b'}} \right) \tag{3}$$

if

$$k_{3b}/k_{1b} = k_{4b}/k_{1b'}$$

then

$$\mathbf{3b}/\mathbf{4b} = k_{D3b}/k_{D4b} \tag{4}$$

Mechanism II: At high temperatures:

$$k_I < k_{con},\ k_{3b}/k_{1b} = k_{4b}/k_{1b'}$$

$$\frac{\mathbf{3b}}{\mathbf{4b}} = \frac{k_{D3b} + k_{D3b'}}{k_{D4b} + k_{D4b'}} \times \frac{\dfrac{K_b}{K_b + 1}}{\dfrac{K_b'}{K_b' + 1}} \tag{5}$$

if

$$\frac{k_{D3b}}{k_{D4b}} = \frac{k_{D3b} + k_{D3b'}}{k_{D4b} + k_{D4b'}}$$

then

$$\frac{\mathbf{3b}}{\mathbf{4b}} = \frac{k_{D3b}}{k_{D4b}} \times \frac{\dfrac{K_b}{K_b + 1}}{\dfrac{K_b'}{K_b' + 1}} \tag{6}$$

When the ratio of k_{3b}/k_{1b} is equal to $k_{4b}/k_{1b'}$, the regioselectivity can be simply determined by the initial double-bond selection (k_{D3b} versus k_{D4b}) by triplet benzophenone (eq 4). If the conformational changes are faster than the ISC processes at high temperatures, $k_I < k_{con}$ (mechanism II), the regioselectivity may be determined by eq 5. Equation 6 can be derived from eq 5 under the condition that the relative rate constant (k_{D3b}/k_{D4b}) is proportional to the total double-bond selection ($k_{D3b} + k_{D3b'}$)/($k_{D4b} + k_{Db'}$). When the switching between the two mechanisms (mechanisms I and II) occurs in the temperature range under investigation, the Eyring plots of the regioselectivity (**3b**/**4b**) should be nonlinear.

To assess the temperature-dependent change of the mechanism, the potential energy surfaces around the dihedral angle θ (deg) of the triplet diradicals, **T-DR3b** and **T-DR4b**, were calculated at the UB3LYP/3-21G level of theory (Figure 6). Again, the outside-gauche conformers (**T-C3b** and **T-C3b′**, θ = ca. 300°) were not calculated to be energy minimum structures, as predicted for **T-DR3a** and **T-DR4a** (Scheme 3). The energy barriers (ΔE_{rel} = ca. 4−8 kcal/mol) between the possible conformers in the triplet diradicals were calculated to be higher than those of **T-DR3a** and **T-DR4a**. The second phenyl substituent derived from benzophenone is responsible for the increase in the energy barriers. The rate constants (k_{con}) for the conformational changes between the equilibrium structures can be estimated to be 10^8 to 10^5 s^{-1} at −70 °C, 10^9 to 10^6 s^{-1} at 25 °C, and 10^{10} to 10^7 s^{-1} at +50 °C. From the lifetime (τ) of the triplet diradicals **T-DR3b** and **T-DR4b** determined by the transient absorption spectra (Figure 4), the ISC rate constant (k_I) of the triplet diradicals ($\tau = 1/k_I$) is determined to be ca. 10^8 s^{-1} at 25 °C. Thus, it is possible that the ISC processes in the triplet diradicals overcome the conformational change between the equilibrium structures at low temperatures, $k_I > k_{con}$ (mechanism I). At high temperatures, mechanism II is operative, since the conformational changes are expected to be faster than the ISC processes ($k_I < k_{con}$).

To assess our hypothetical mechanism, the theoretical ratios of ln(**3b**/**4b**) calculated by eq 4 (green line, mechanism I) and eq 6 (blue line, mechanism II) were plotted against the inverse of reaction temperatures (Figure 7). The activation parameters $\Delta\Delta H^{\ddagger}$ and $\Delta\Delta S^{\ddagger}$ (Figure 7a,d) for the double-bond selection, k_{D3b}/k_{D4b}, were calculated from the product ratios of **3b**/**4b** observed below the temperature of −55 °C for **2a** and −50 °C for **2b**. The entropy-controlled selections, i.e., k_{D3b}/k_{D4b}, are consistent with the early transition state of bond-forming steps of the energy-rich nπ^*-**1b** with furans (Figure 7a,d).[31] The equilibrium constants K_b in **T-DR3b** and K_b' in **T-DR4b** were calculated from the computed energy differences, $\Delta G = \Delta H - T\Delta S$, between the equilibrium conformers. As for the diradicals formed in the reaction with 2-methylfuran (**2a**), the population of the productive conformer **T-C1ba′** in **T-DR4ba** is calculated to be *higher* than that of the productive conformer **T-C1ba** in **T-DR3ba**, i.e., $K_b' > K_b > 1$ (Figure 6a,b, Scheme 5). Thus, under the conditions of mechanism II ($k_{con} > k_I$), higher substituted oxetane **4ba** is expected to form more than the chemical yield anticipated from the initial double-bond selection (**T-DR3ba**/**T-DR4ba**, mechanism I). Consistent with this prediction, the Eyring plot (Figure 7b, red line) that was experi-

(31) (a) Skell, P. S.; Cholod, M. S. *J. Am. Chem. Soc.* **1969**, *91*, 7131. (b) Giese, B. *Angew. Chem., Int. Ed.* **1977**, *16*, 125. (c) Bach, T.; Jodicke, K.; Kather, K.; Frohlich, R. *J. Am. Chem. Soc.* **1997**, *119*, 2437.

Scheme 4. Mechanism for the Formation of Oxetanes **3** and **4** in the PB Reaction of Furans **2** with Benzophenone (**1b**)

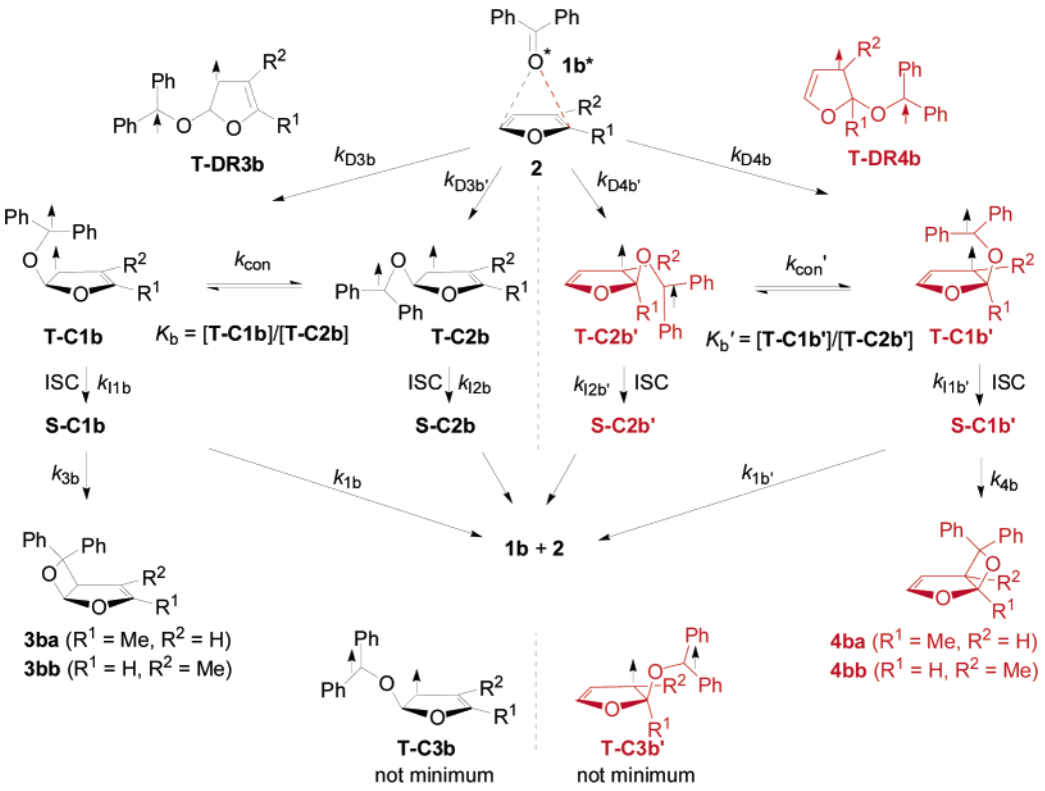

mentally obtained departs from the green line (Figure 7a, mechanism I) at ca. −55 °C with the increase in the reaction temperature and approaches to the blue line (Figure 7c, mechanism II). As for the regioselectivity in the reaction with 3-methylfuran (**2b**) (Figure 7d−f), since the population of the productive conformer **T-C1bb′** in **T-DR4bb** is calculated to be *lower* than that of the conformer **T-C1bb** in **T-DR3bb**, $K_b > 1$, $K_b' < 1$ (Scheme 4), at high temperature lower substituted oxetane **3bb** is expected to form more than the chemical yield anticipated from mechanism I (**T-DR3bb**/**T-DR4bb**). Thus, the Eyring plot (Figure 7e, red line) departs from the green line (Figure 7d) with increase in the temperature, and approaches the blue line (Figure 7f) plotted according to eq 6 (mechanism II). The decrease in the quantum yield at high temperature, $\Phi_{3+4} = 0.39$ at −77 °C → 0.06 at +56 °C, supports the mechanism.

The contrastive difference between the population of productive conformers **T-C2ba′** and **T-C2bb′** in **T-DR4b** can be reasonably explained by steric effect (Scheme 5). Since the steric repulsion between the methyl and the diphenylmethyl group is significant in **T-C2ba′**, the conformer **T-C1ba′** is more stable in **T-DR4ba** ($\Delta E_{rel} = -3.1$ kcal/mol). In contrast, the conformer **T-C2bb′** is a more favorable structure than **T-C1bb′** ($\Delta E_{rel} = +1.1$ kcal/mol), since the steric repulsion between the methyl and diphenylmethyl group is severer than that between the hydrogen and the diphenylmethyl group. The equilibrium constant (K_b) between **T-C1b** and **T-C2b** ($\Delta E_{rel} = -1.0$ kcal/mol) is not dependent on the position of the methyl group, since the methyl substituent is located far from the diphenylmethyl group.

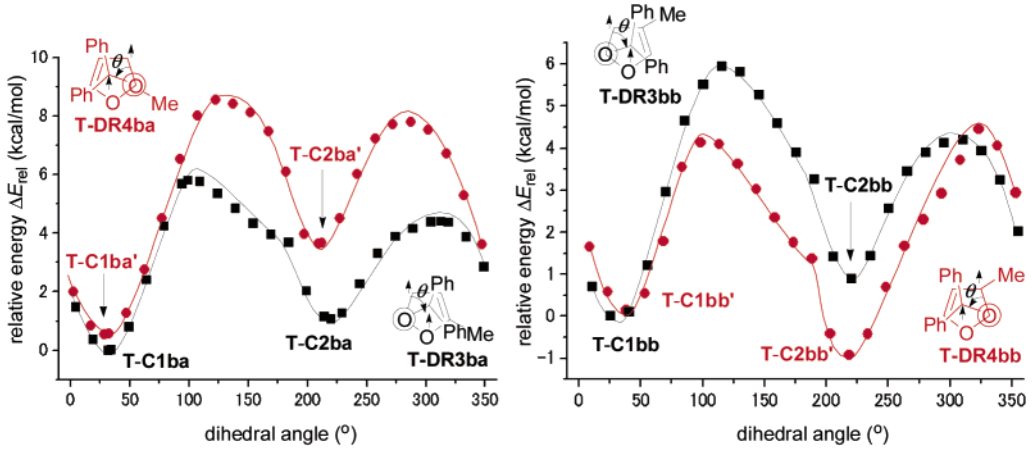

Figure 6. PES analyses around the dihedral angle (θ°) in diradicals (a) **T-DR3ba**, (b) **T-DR4ba**, (c) **T-DR3bb**, and (d) **T-DR4bb**. The total electronic energies, ΔE_{rel} in kcal/mol, were relative to the most stable conformer.

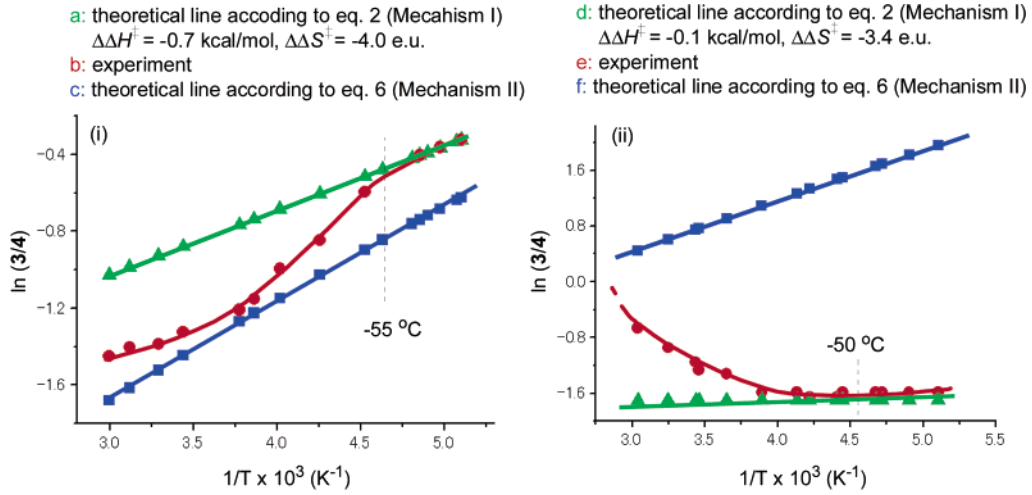

Figure 7. Theoretical and experimental plots of ln(**3**/**4**) against 1/*T* in the PB reaction of benzophenone (**1b**) with (i) 2-methylfurane (**2a**) and (ii) 3-methylfuran (**2b**).

Scheme 5. Steric Effect on the Equilibrium Constants K_b and K_b' in Triplet 1,4-Diradicals **T-DR4ba** and **T-DR-4bb**

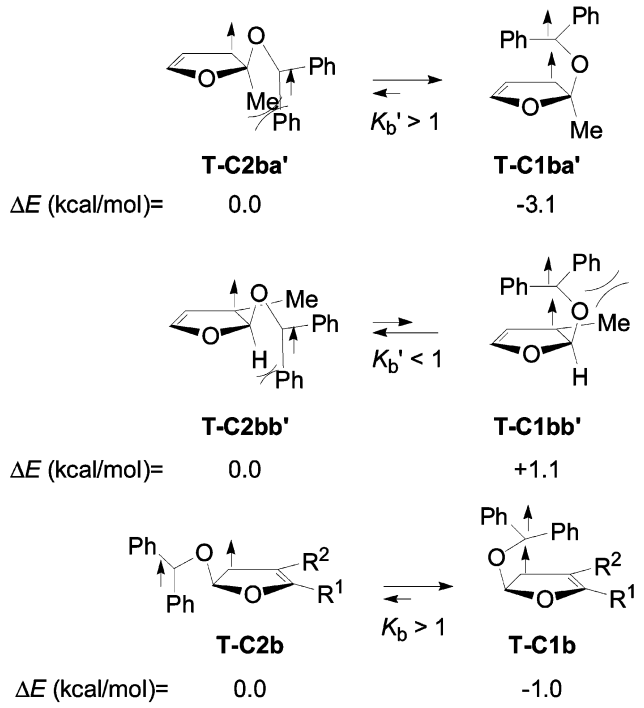

In summary, we found unusual temperature[32] and substituent effects on the stereo- and regioselectivity in the PB reaction of furan derivatives. The experimental and computational results have provided convincing evidence regarding the mechanism of these reactions, which has been debated until now. The conformational distributions of the intermediary triplet 1,4-diradicals, which are controlled by the gauche effect and the steric effect, play a crucial role to determine the stereo- and regioselectivity. Thus, the energetic preference of the inside-gauche conformers in intermediary triplet diradicals was proposed to be responsible for the exclusive formation of exo-oxetanes **3a** and **4a** in the reactions with benzaldehyde. The nonlinear Eyring plots observed in the reactions with benzophenone is reasonably explained by the switching between mechanisms I and II in the temperature range under investigations. These fundamental findings on the reaction mechanism provide valuable information to predict the selectivities in other Paternò−Büchi reactions.

(32) Unusual temperature effect on the diastereoselectivity was observed in the PB reaction of cyclooctene with ketones. See: Adam, W.; Stegmann, V. R. *J. Am. Chem. Soc.* **2002**, *124*, 3600.

Experimental Section

General Procedure for the Photoreactions of Aromatic Carbonyl Compounds with Furan Derivatives. A degassed toluene solution of freshly distilled furan **2** (0.5 M, 5 mmol) and aromatic carbonyl compound **1** (0.05 M, 0.5 mmol) was irradiated for 30 min with a high-pressure Hg lamp through a Pyrex filter at various temperatures. After the solvent was removed under the reduced pressure by using a vacuum pump (0.2 mmHg, <10 °C), the photolyzate was directly analyzed by ^{1}H NMR (270 and 600 MHz) spectroscopy. The spectra revealed the quantitative formation of the bicyclic oxetanes **3** and **4** together with excess amount of aromatic carbonyls. The product ratios were determined by the comparison of the peak areas, error <3%. The photoproducts **3** and **4** were isolated by using alumina column chromatography. Some decomposition of the oxetanes was observed during the column chromatography. The oxetanes were decomposed to unidentified products on silica gel column chromatography. Although bicyclic oxetanes **3aa**,[3a] **4aa**,[3a] **4ba**,[3b,d] **3bb**[3b,d] are known compound, the high-resolution spectra were not available. ^{1}H NMR spectra (270 or 600 MHz) for the compounds are listed below, together with the new compounds **3ab**, **4ab**, **3ba**, and **4bb** assigned in this study.

3-Methyl-6-phenyl-2,7-dioxabicyclo[3.2.0]hept-3ene (*exo*-3aa).[3a] ^{1}H NMR (600 MHz, $CDCl_3$): δ 2.00 (s, 3 H), 3.62−3.65 (m, 1 H), 5.08−5.10 (m, 1 H), 5.54 (d, J = 3.0 Hz, 1 H), 6.50 (d, J = 4.6 Hz, 1 H), 7.24−7.43 (m, 5 H).

1-Methyl-6-phenyl-2,7-dioxabicyclo[3.2.0]hept-3ene (*exo*-4aa).[3a] ^{1}H NMR (600 MHz, $CDCl_3$): δ 1.73 (s, 3 H), 3.42−3.43 (m, 1 H), 5.38−5.40 (m, 1 H), 5.51 (d, J = 3.6 Hz, 1 H), 6.63 (d, J = 3.0 Hz, 1 H), 7.21−7.42 (m, 5 H).

3-Methyl-6,6-diphenyl-2,7-dioxabicyclo[3.2.0]hept-3ene (3ba). ^{1}H NMR (270 MHz, $CDCl_3$): δ 2.29 (s, 3 H), 4.30−4.32 (m, 1 H), 4.51−4.52 (m, 1 H), 6.22 (d, J = 4.6 Hz, 1 H), 7.11−7.76 (m, 10 H); ^{13}C NMR (67.8 MHz, $CDCl_3$): δ 13.7, 57.1, 90.7, 97.4, 105.2, 125.3, 125.4, 126.7, 127.1, 127.8, 143.0, 145.3; IR (liquid film): 3106−2926, 1612, 1491, 1452, 1396, 1136 cm^{-1}; Anal. Calcd for $C_{18}H_{16}O_2$: C, 81.79; H, 6.10. Found: C, 81.60; H, 6.40.

1-Methyl-6,6-diphenyl-2,7-dioxabicyclo[3.2.0]hept-3ene (4ba).[3b,d] ^{1}H NMR (270 MHz, $CDCl_3$): δ 1.57 (s, 3 H), 4.16 (d, J = 1.0 and 3.0 Hz, 1 H), 4.90 (t, J = 3.0 Hz, 1 H), 6.39 (dd, J = 1.0 and 3.0 Hz, 1 H), 7.15−7.51 (m, 10 H).

4-Methyl-6-phenyl-2,7-dioxabicyclo[3.2.0]hept-3ene (*exo*-3ab). ^{1}H NMR (270 MHz, $CDCl_3$): δ 1.79 (s, 3 H), 3.47−3.49 (m, 1 H), 5.57 (d, J = 3.0 Hz, 1 H), 6.37 (s, 1 H), 6.48 (d, J = 4.3 Hz, 1 H), 7.31−7.46 (m, 5 H); ^{13}C NMR (67.8 MHz, $CDCl_3$): δ 9.5, 55.9, 91.1, 108.6, 113.9, 125.0, 128.1, 128.8, 141.3, 141.9; IR (liquid film, with **4ab**): 3111−2912, 1634, 1453, 1387 cm^{-1}; Anal. Calcd for $C_{12}H_{12}O_2$ (with **4ab**): C, 76.57; H, 6.43. Found: C, 76.22; H, 6.45.

5-Methyl-6-phenyl-2,7-dioxabicyclo[3.2.0]hept-3ene (*exo*-4ab). ^{1}H NMR (270 MHz, $CDCl_3$): δ 0.81 (s, 3 H), 5.37 (d, J = 2.7 Hz, 1 H), 5.66 (s, 1 H), 6.11 (s, 1 H), 6.63 (d, J = 2.7 Hz, 1 H), 7.31−7.46 (m, 5 H); ^{13}C NMR (67.8 MHz, $CDCl_3$): δ 15.8, 56.1, 94.6, 110.9, 111.6, 125.2, 128.7, 128.9, 139.2, 146.8.

4-Methyl-6,6-diphenyl-2,7-dioxabicyclo[3.2.0]hept-3ene (3bb). ^{1}H NMR (270 MHz, $CDCl_3$): δ 1.95 (s, 3 H), 4.10 (d, J = 4.3 Hz, 1 H), 6.05 (d, J = 4.3 Hz, 1 H), 6.12 (s, 1 H), 7.21−7.87 (m, 10 H); ^{13}C NMR (67.8 MHz, $CDCl_3$): δ 18.6, 61.1, 96.6, 108.3, 109.9, 125.3, 125.9, 127.2, 127.7, 128.3, 128.4, 142.9, 143.8, 145.4; IR (KBr, with **4bb**): 2867−3225, 1657, 1560, 1396 cm^{-1}; Anal. Calcd for $C_{18}H_{16}O_2$: C, 81.79; H, 6.10. Found: C, 81.60; H, 6.08.

5-Methyl-6,6-diphenyl-2,7-dioxabicyclo[3.2.0]hept-3ene (4bb).[3b,d] ^{1}H NMR (270 MHz, $CDCl_3$): δ 1.10 (s, 3 H), 5.01 (d, J = 2.7 Hz, 1 H), 5.96 (s, 1 H), 6.15 (d, J = 2.7 Hz, 1 H), 7.21−7.87 (m, 10 H).

Determination of Quantum Yields of Oxetane Formations. The quantum yields of the oxetane formations in the photoreaction of aromatic carbonyl with furan derivatives were measured by Xenon lamp focused at 313 nm. The absorbance at 313 nm of a solution of the sample remained above 1.5 during the irradiation, and thus, no correction for transmitted light was necessary. The intensity of the light source was determined on the basis of the known quantum yield for the Norrish type-II photochemical decomposition of valerophenone (Φ_{PhCOMe} = 0.33 at 313 nm).[33] The obtained values in the text are the average after three trials, error <10%.

Transient Absorption Spectroscopic Measurement. Picosecond[34] time-resolved difference spectra were obtained by using the third harmonic of a mode-locked Nd^{3+}:YAG laser (Continuum PY61C-10, λ_{exc} = 355 nm) for excitation. The transient absorption spectra in the time range from 20 ps to 6 ns were acquired by using continuum pulses with delays of 20−6000 ps. The latter was generated by focusing the fundamental laser pulse into a flowing H_2O/D_2O mixture (1:1 by volume).

Acknowledgment. We thank Mrs. T. Muneishi at the Analytical Center of Faculty of Engineering, Osaka University, for measuring the 600 MHz NMR spectra.

Supporting Information Available: Computational details (PDF). This material is available free of charge via the Internet at http://pubs.acs.org.

JA039491O

(33) Wagner, P. J.; Kemppainen, A. E. *J. Am. Chem. Soc.* **1968**, *90*, 5896.
(34) Ohno, T.; Nozaki, K.; Haga, M. *Inorg. Chem.* **1992**, *31*, 548.